Dalton Transactions

ROYAL SOCIETY OF CHEMISTRY

PERSPECTIVE

View Article Online
View Journal | View Issue

Check for updates

Cite this: *Dalton Trans.*, 2022, **51**, 13145

Inorganic material-based Janus nanosheets: asymmetrically functionalized 2D-inorganic nanomaterials

Ryoko Suzuki, [a,b] Yusuke Yamauchi [a,c,d] and Yoshiyuki Sugahara *[a,d,e]

Received 19th May 2022,
Accepted 26th July 2022

DOI: 10.1039/d2dt01557a

rsc.li/dalton

During the past decade, various inorganic material-based Janus nanosheets have been prepared and their applications have been proposed. Inorganic material-based Janus nanosheets have various advantages over polymer-based Janus nanosheets, including the maintenance of their characteristic two-dimensional shape, and are expected to be applied as unique functional materials. Methods for regioselective functionalization of the two sides of the individual nanosheets are extremely important for the development of inorganic material-based Janus nanosheets. In this review, the preparation methods and applications of inorganic material-based Janus nanosheets are summarized from the point of view of inorganic nanosheet functionalization.

Open Access Article. Published on 23 2022. Downloaded on 08.12.2025 15:29:53.
This article is licensed under a Creative Commons Attribution-NonCommercial 3.0 Unported Licence.

Introduction

Inorganic nanosheets are high-aspect-ratio materials, typically with single-nanometer thicknesses and a lateral size of several micrometers. To date, nanosheets made from various materials, such as clay minerals, graphite, alkoxysilanes and layered transition metal oxides, have been applied as fillers,[1] electronic materials[2] and magnetic materials.[3] Their surfaces are often modified to improve their properties and introduce new functions.[4–6] There have been many reports about the surface modification of inorganic nanosheets using functional organic compounds, such as surface modifiers with hydrophobic groups,[5,7,8] ionic liquid moieties[9,10] and polymeric chains.[4,11] The majority of these studies achieved uniform surface modification of inorganic nanosheets using one type of surface modifier. Recently, Janus nanosheets have been prepared by regioselective surface modification of the two sides of individual inorganic nanosheets, taking advantage of their high anisotropy.

Janus materials are unique materials characterized by distinct surfaces with two different chemical properties. Since the introduction of the "Janus grains" concept in 1991,[12] many types of Janus materials with various compositions and shapes have been prepared and applied experimentally as surfactants, catalysts and optical materials.[13–15] These materials are variously classified as zero-dimensional materials such as nanoparticles, one-dimensional materials such as nanowires and nanorods, and two-dimensional materials such as nanosheets. Among these Janus materials, Janus nanosheets have the highest anisotropy and exhibit several properties such as high adsorption energy at interfaces due to their shapes. Janus nanosheets have been classified as either polymer-based Janus nanosheets or inorganic material-based Janus nanosheets. Among them, inorganic material-based Janus nanosheets have the advantage of maintaining their shapes in various solvents, leading to extension of their applications in various fields.[16]

In this review, we have focused on inorganic material-based Janus nanosheets, which are defined as individual single-layered nanosheets bearing two types of lateral surfaces with different properties. Inorganic material-based Janus nanosheets are further classified into two categories. The materials in one category have Janus structures in inorganic nanosheets themselves. The materials in the other category comprise individual nanosheets possessing two different surfaces achieved *via* surface functionalization. Janus-transition-metal dichalcogenide nanosheets are assigned to the former category.[17,18] Compositions in the crystal structures of tran-

[a]*Kagami Memorial Research Institute for Science and Technology, Waseda University, 2-8-26, Nishi-waseda, Shinjuku-ku, Tokyo 169-0051, Japan. E-mail: ys6546@waseda.jp*
[b]*Nikon Corporation, 1-10-1, Asamizodai, Minami-ku, Sagamihara, Kanagawa 252-0328, Japan*
[c]*School of Chemical Engineering and Australian Institute for Bioengineering and Nanotechnology (AIBN), The University of Queensland, Brisbane, QLD 4072, Australia*
[d]*International Center for Materials Nanoarchitectonics (WPI-MANA), National Institute for Materials Science (NIMS), 1-1 Namiki, Tsukuba, Ibaraki 305-0044, Japan*
[e]*Department of Applied Chemistry, School of Advanced Science and Engineering, Waseda University, 3-4-1, Okubo, Shinjuku-ku, Tokyo 169-8555, Japan*

Open Access Article. Published on 23 2022. Downloaded on 08.12.2025 15:29:53.
This article is licensed under a Creative Commons Attribution-NonCommercial 3.0 Unported Licence.

sition-metal dichalcogenide nanosheets are asymmetric, and their electric structures were investigated by advanced characterization techniques and simulations. Furthermore, Janus nanosheets consisting of TiO_2 and ZnO surfaces were prepared by peeling off stacked TiO_2 and ZnO layers formed by atomic layer deposition (ALD) from a polymer substrate.[19] Inorganic material-based Janus nanosheets in the second category were prepared by regioselective functionalization of two-dimensional materials, including silica,[16,20–23] graphene[24–32] and clay minerals.[33–35] It should be noted that the inorganic material-based Janus nanosheets in the latter category provide a large number of choices in terms of variation in functions and, therefore, in applications as compared to the inorganic material-based Janus nanosheets in the former category.

In this review, several strategies for regioselective introduction of functional groups on nanosheet surfaces and design of new functions through selection of surface functional groups for inorganic material-based Janus nanosheets in the latter category are summarized. This review is divided into (1) silica-based Janus nanosheets, (2) graphene-based Janus nanosheets, and (3) other Janus nanosheets based on clay minerals and ion-exchangeable layered materials (Fig. 1). These three types of inorganic material-based Janus nanosheets were categorized according to their chemical composition: silica-based Janus nanosheets composed of two-dimensional networks formed from silicon and oxygen; graphene-based Janus nanosheets composed mainly of carbon; and a third type of Janus nanosheet, clay mineral-based Janus nanosheets composed of clay nanosheets formed mainly from silicon, aluminum, and oxygen. Janus nanosheets have also been prepared from ion-exchangeable layered materials, including $K_4Nb_6O_{17}{\cdot}3H_2O$ and MXene, which are composed of nanosheets formed from various elements, including titanium, niobium, carbon, fluorine, oxygen and hydrogen. Various applications using Janus nanosheets and their future prospects are also addressed.

Silica-based Janus nanosheets

The sol–gel process using alkoxysilanes has been an important synthesis method for the preparation of various materials, such as glasses,[36] fibers,[37] thin films,[38] nanoparticles,[39] mesoporous silicas[40] and polyhedral oligomeric silsesquioxanes (POSSs).[41] Si–O–Si bonds are formed *via* hydrolysis and condensation of alkoxysilanes.[42] Silica-based Janus nanosheets have been prepared using the sol–gel process. The basic preparation strategy for producing a nanosheet morphology consists of self-assembly of organotrialkoxysilanes at liquid–liquid or solid–liquid interfaces, formation of Si–O–Si bonds by the sol–gel process and crushing of the resultant hollow particles. Several organotrialkoxysilanes were simultaneously or sequentially reacted for the preparation of regioselectively functionalized silica layers, leading to silica nanosheets with Janus structures.

Silica-based Janus nanosheets were the first examples of inorganic material-based Janus nanosheets. Nanosheet formation and masking can be achieved by self-assembly of silica sources, such as organotrialkoxysilanes, on oil droplet surfaces in emulsions or particulate template surfaces.[16,20–23] Therefore, it was necessary to use silica sources which could be adsorbed on template or droplet surfaces. Since many types of alkoxysilanes are commercially available, silica-based Janus nanosheets with various functionalities have been prepared. One of the potential advantages for silica-based Janus nanosheets is the controllability of their shapes and thicknesses *via* changes in the sol–gel reaction conditions, a characteristic difference from other inorganic material-based Janus nanosheets prepared by surface modification of layered materials.

Liang *et al.* first reported the preparation of a silica-based Janus nanosheet.[16] First, an emulsion was prepared using water and paraffine and containing tetraethyl orthosilicate (TEOS), aminopropyltrimethoxysilane (APTMS) and phenyltriethoxysilane (PTES). Subsequently, a sol–gel reaction was conducted at 70 °C. At this stage, TEOS formed the frame of a silica shell at the interface on paraffine droplets in an emul-

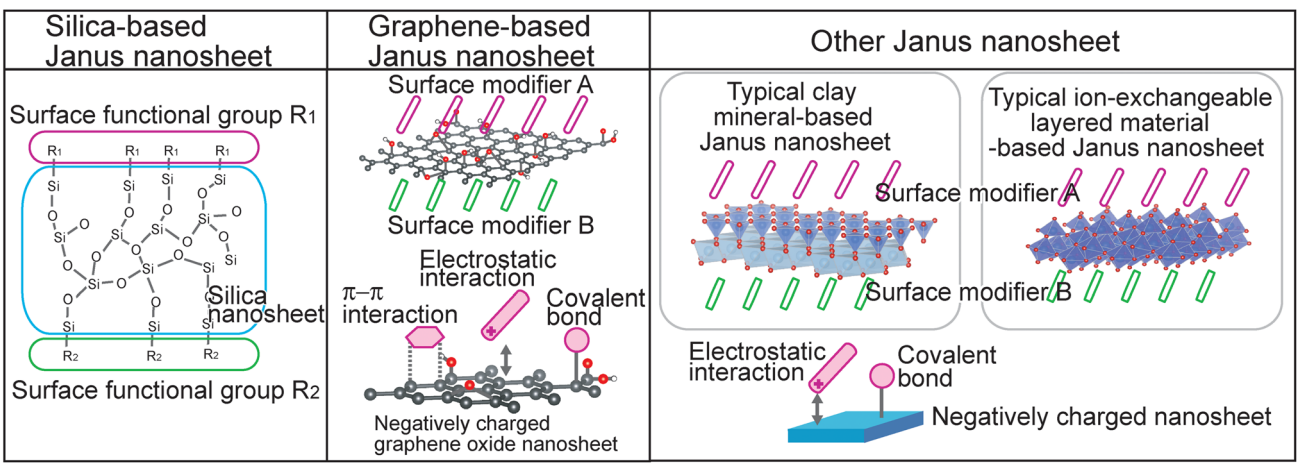

Fig. 1 Structural models of silica-based Janus nanosheets, graphene-based Janus nanosheets and other Janus nanosheets, which exhibited typical nanosheets.

 This journal is © The Royal Society of Chemistry 2022

Open Access Article. Published on 23 2022. Downloaded on 08.12.2025 15:29:53.
This article is licensed under a Creative Commons Attribution-NonCommercial 3.0 Unported Licence.

sion, and a phenyl group of PTES and the amino group of APTMS spontaneously orientated to the paraffine phase and the aqueous phase at the interface, respectively. The paraffine core was then removed by its dissolution in hexane. Finally, silica-based Janus nanosheets with phenyl groups on one side and amino groups on the other side of the individual silica nanosheets were obtained by crashing the silica shell-bearing phenyl group and aminopropyl group on the inner and outer surfaces, respectively (Fig. 2a). The thickness of silica-based Janus nanosheets could be controlled by changing the sol–gel reaction time. The thickness of a representative silica-based Janus nanosheet was 65 nm.

The above-mentioned silica-based Janus nanosheets were hardly adsorbed onto the curved surface, since they were thick and rigid nanosheets. Thus, ultra-thin Janus nanosheets with flexibility were prepared[20] using $CaCO_3$ particles as a template instead of oil droplets in an emulsion. First, 3-butyldianhydride mercaptopropyltrimethoxysilane (BDMPS) was assembled on $CaCO_3$ particles *via* adsorption of a monolayer, with an acid anhydride group in BDMPS on the $CaCO_3$ particle surface and Si–OMe groups exposed to the outer surface. Si–O–Si bonds were formed *via* hydrolysis and condensation of the Si–OMe groups of BDMPS, followed by modification of the Si–O–Si surface with octadecyltrichlorosilane. Finally, silica-based Janus nanosheets were prepared through etching of $CaCO_3$ particles by ultrasonication under acidic conditions. The thickness of this type of Janus nanosheet was decreased to 3.5 nm.

The shapes of the above two Janus nanosheets were not controlled, since a silica shell crushing process was involved. Xue *et al.* successfully prepared shape-controlled silica-based Janus nanosheets.[21] Ag particles were deposited on SiO_2 shells by reduction of $AgNO_3$ for core–shell particle formation. Then, *n*-octyltrimethoxysilane was reacted with the obtained particles, followed by HNO_3 treatment for dissolving the Ag particles. The hollow particles obtained had two areas, one with a SiO_2 surface reflecting the shape of the Ag particles and the other with exposed surface octyl groups. While the octyl-group-modified surface was not reacted during further processing, the SiO_2 surface was reacted with 4-(chloromethyl)phenyltrimethoxysilane ($PhCH_2Cl$-TMS), followed by oxidation of the $PhCH_2Cl$ group. Particles with patchy PhCHO group areas were obtained. Then, imine bonds were formed by a reaction of APTMS with the PhCHO group. At this stage, the APTMS moiety formed patchy domains reflecting the shape of the Ag particles. A single-layered silsesquioxiane shell was obtained by formation of Si–O–Si bonds *via* the homocondensation of APTMS. Finally, Janus nanosheets bearing an aminopropyl moiety on one side were obtained by breaking the imine bonds under acidic conditions. The shape of Janus nanosheets could be controlled by controlling the shape of the Ag particles, since the Janus nanosheets reflected the shape of the Ag particles. Also, the size of the Ag particles was controlled by changing the time period for Ag particle generation. This is a unique preparation method which could control both the shape and thickness of inorganic material-based Janus nanosheets.

Furthermore, mesoporous silica-based Janus nanosheets were prepared.[22] Inorganic material-based Janus nanosheets could be separated into two phases, such as water and oil phases. Separation of the two phases caused some problems, however, such as restriction of mass transfer during the catalytic reaction. Thus, Yan *et al.* proposed the use of mesoporous silica nanosheets as base materials for Janus nanosheets. Mesoporous silica prepared using a surfactant as a template was coated on polystyrene (PS) particles. Then, the products were modified using *n*-octyltrimethoxysilane bearing a hydrophobic group. Finally, the PS particles were dissolved in tetrahydrofuran (THF) and removed. Furthermore, Pd nanoparticles were loaded onto the porous surface of the obtained mesoporous silica-based Janus nanosheets, and the resulting Janus nanosheets exhibited high catalytic activity upon aqueous nitroarene reduction.

Yin *et al.* developed a preparation method for silica-based Janus nanosheets with high productivity.[23] Cross-linked polyacrylamide particles were used as a template in this method. First, organotrialkoxysilanes which could be adsorbed on a polyacrylamide template were screened using computer simulation. As a result, γ-ureidopropyltrimethoxysilane (UPS) and 3-butyldianhydride mercaptopropyltrimethoxysilane (BDMPS) were selected for the preparation of silica-based Janus nanosheets. They were adsorbed onto polyacrylamide particles, and Si–O–Si bonds were formed by a sol–gel reaction of Si–OMe groups in UPS and BDMPS on the outer surfaces of the particles. The outer surfaces of the resulting particles were further modified using octadecyltrichlorosilane. Janus nanosheets were then obtained by removing the silica shell from the polyacrylamide surface using ultrasonication (Fig. 2b). The templates, polyacrylamide particles, were reusable since they were not dissolved during the process.

There are a large number of reports about silica-based Janus nanosheets in addition to those mentioned above. Also,

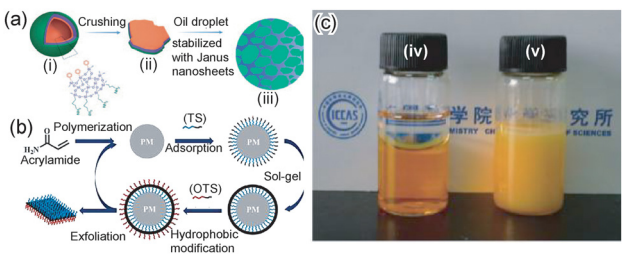

Fig. 2 (a) Scheme of the preparation of silica-based Janus nanosheets. Core–shell particles were formed by the self-assembly of three types of silica source and the sol–gel process at the water–oil interface in an emulsion. (i) After dissolution of the oil core, hollow silica spheres were formed. (ii) Silica-based Janus nanosheets were obtained by crushing the hollow silica spheres. (iii) The obtained silica-based Janus nanosheets can be used as a solid surfactant.[16] Adapted with permission from ref. 16. Copyright 2011 John Wiley and Sons. (b) Scheme of the preparation of silica-based Janus nanosheets *via* a reusable polyacrylamide microsphere template.[23] Adapted with permission from ref. 23. Copyright 2019 Elsevier. (c) (iv) An immiscible mixture of toluene (top) and water (bottom) and (v) a water-in-toluene emulsion stabilized with silica-based Janus nanosheets containing 69.6 wt% PDVB.[43] Adapted with permission from ref. 43. Copyright 2012 American Chemical Society.

Open Access Article. Published on 23 2022. Downloaded on 08.12.2025 15:29:53.
This article is licensed under a Creative Commons Attribution-NonCommercial 3.0 Unported Licence.

various applications for silica-based Janus nanosheets such as surfactants,[43–52] catalysts[53–61] and materials for polymer blends[62–65] have been investigated. The most common application is utilization as surfactants. Silica-based Janus nanosheets bearing hydrophilic and hydrophobic surfaces can function as two-dimensional surfactants. Also, the hydrophobicity and hydrophilicity of silica-based Janus nanosheets can be controlled by the composition of dispersant media, temperature and light using ionic liquids and stimuli-responsive polymers as functional groups. Thus, the versatility of functional groups is an advantage of organoalkoxysilanes, since various types of organoalkoxysilanes are commercially available.

Chen *et al.* reported the control of the balance between the hydrophobicity and hydrophilicity of silica-based Janus nanosheets.[43] The self-assembly of organoalkoxysilanes at the water–oil interface of an O/W emulsion was used in the preparation process. A monomer; divinylbenzene (DVB), a polymerization initiator; azodiisobutyronitrile (AIBN) and three types of alkoxylsilanes; TEOS, 3-methacryloxypropyltrimethoxysilane (MPS) and APTES were dissolved in *n*-decane, an oil phase. By initiating a sol–gel reaction, a silica shell whose inner and outer surfaces had a methacrylic group and an amino group, respectively, was formed. Since methacrylic groups faced the oil phase containing a monomer and a polymerization initiator, polydivinylbenzene (PDVB) chains were grown on the inner surface of the silica shell. Finally, the silica shell was crushed and silica-based Janus nanosheets bearing hydrophilic amino groups on one side and a hydrophobic PDVB layer on the other side were obtained. The polymer content in the Janus nanosheets could be controlled by changing the amount of the monomer in the oil phase. A water–toluene emulsion was stabilized using Janus nanosheets that contained 69 wt% PDVB (Fig. 2c).

Moreover, Yang *et al.* reported pH-responsive Janus nanosheets.[44] Janus nanosheets bearing an *n*-octyltriethoxysilane moiety and poly (2-(dimethylamino)ethyl methacrylate) (PDEAEMA) chains separately on the two sides of the individual nanosheets were prepared. Since the pK_a of PDEAEMA is 7.2, the polymer chains were positively charged at low pH and the PDEAEMA surface exhibited hydrophilicity. On the other hand, the PDEAEMA surface exhibited hydrophobicity at high pH. Due to this behavior, the stability of the emulsion could be controlled by adjusting the pH.

There were several reports concerning stimuli-response Janus nanosheets. Janus nanosheets with pH-responsive PDEAEMA chains on one side and poly(*N*-isopropylacrylamide) (PNIPAAm) chains on the other side were reported.[45] Also, the balance of the hydrophobicity and hydrophilicity of Janus nanosheets was controlled by light-responsive polymer chains.[46] Since these Janus nanosheets allow control of their hydrophobicity and hydrophilicity based on the response of polymer chains to stimuli, they are expected to find applications as smart materials.

Silica-based Janus nanosheets have also been applied as catalysts. Janus nanosheets improved the efficiency of catalytic reactions by increasing the stability of two-phase reaction systems and promoting mass transfer. In a degradation reaction of water-soluble methyl orange,[53] degradation products were insoluble in water. Therefore, a biphasic system, which enables methyl orange and a degradation product to be present in a water phase and an oil phase, respectively, is suitable for the reaction. Silica-based Janus nanosheets with a $PW_{12}O_{40}^{3-}$ moiety that has catalytic activity with methyl orange degradation on one side and a phenyl moiety separately on the other side were prepared. An emulsion was formed using water to dissolve methyl orange, toluene and the Janus nanosheets. At the interface of oil droplets in the emulsion, the Janus nanosheet surface bearing the $PW_{12}O_{40}^{3-}$ moiety faced the aqueous phase. Methyl orange was degraded and degradation products diffused to the oil phase. The degradation rates of methyl orange for the emulsion containing the Janus nanosheets and water containing the Janus nanosheets were 99.2% and 88.4%, respectively, demonstrating that the reaction efficiency was improved by the presence of catalytic Janus nanosheets at the water–oil interphase. In another study, silica-based Janus nanosheets bearing a phenyl moiety on one side and TiO_2 particles deposited on the other side were used for the degradation of a water-soluble dye, malachite green.[54] The contact areas between the TiO_2-deposited surface of the Janus nanosheets and malachite green were increased by forming an emulsion leading to an increase in catalytic activity. Also, Xu *et al.* reported the catalytic activity of silica-based Janus nanosheets bearing a phenyl moiety on one side and Au particles deposited on the other side.[55] In a water–oil biphasic reductive reaction of *p*-nitroanisole, the Janus nanosheets exhibited higher reaction efficiency than a Janus silica-particle catalyst that was covered with two types of polymer chains in two areas of the individual silica particles featuring one polymer surface loaded with Au nanoparticles.[56] This result indicates that Janus nanosheets promote catalytic reactions more efficiently when the interfaces are stabilized. Such silica-based Janus nanosheets with functions as an emulsifier and a catalyst were reported in other studies[57–61] and they exhibited higher efficiency in catalytic reactions than other catalysts without Janus structures.

There has been very limited application of Janus nanosheets as a filler for self-healing hydrogels.[66] Silica-based Janus nanosheets bearing polydopamine (PDA) and 2-(3-(6-methyl-4-oxo-1,2,3,4-tetrahydropyrimidin-2-yl)ureido)ethyl methacrylate (MAUPy), where both functional groups formed a large number of hydrogen bonds on separately either side were added into self-healing hydrogels. The hydrogen bonds in MAUPy improved the self-healing property of the composite hydrogel. The mechanical strength of the composite hydrogel was also improved.

Graphene-based Janus nanosheets

In a difference from silica-based Janus nanosheets, graphene-based Janus nanosheets do not require formation from precur-

 This journal is © The Royal Society of Chemistry 2022

Open Access Article. Published on 23 2022. Downloaded on 08.12.2025 15:29:53.
This article is licensed under a Creative Commons Attribution-NonCommercial 3.0 Unported Licence.

sors. Masking and regioselective surface modification of exfoliated graphene nanosheets are important techniques for the preparation of graphene-based Janus nanosheets. There are various exfoliation methods for graphite, which consists of stacked graphene nanosheets. Among these, Hummers' method, which promotes the exfoliation of graphite by two-dimensional structure surface oxidation using H_2SO_4, $NaNO_3$ and $KMnO_4$,[67] is the most common method. The surfaces of the graphene oxide (GO) nanosheets obtained possess hydroxyl groups, epoxy groups and carboxy groups. These surface functional groups could be used as active sites for further surface modification.[68,69]

The first report of the preparation of graphene-based Janus nanosheets employed a dry process.[24] Single-layered GO nanosheets were deposited on a substrate and reacted with chlorine gas for single-sided surface modification by chlorine molecules. Poly(methyl methacrylate) (PMMA) was coated on the Cl-modified graphene. By peeling off the PMMA film from the substrate, the unmodified graphene surface was modified using benzoyl peroxide for phenylation. Finally, graphene-based Janus nanosheets were obtained by dissolving the PMMA film with acetone. Deposition of graphene on a substrate resulted in masking of the unexposed side of graphene, and regioselective surface modification of graphene was achieved (Fig. 3a).

Graphene-based Janus nanosheets were also prepared in an emulsion in a way similar to that used for the preparation of silica-based Janus nanosheets.[25] A Pickering emulsion was prepared with melted wax droplets whose surface was covered with multi-layered GO nanosheets and water. Wax droplets coated with multi-layered GO nanosheets were washed using an NaOH aqueous solution for removing excess stacked GO nanosheets. The outer surfaces of single-layered GO nanosheets adsorbed onto wax droplets were modified using poly(propylene glycol)bis(2-aminopropyl ether) with an average molecular weight of ~2000 (D2000) or dodecylamine (DDA). Graphene-based Janus nanosheets were obtained by dissolving the wax droplets in ethanol. In this study, masking of one side of individual GO nanosheets was achieved by their adsorption onto wax droplets (Fig. 3b).

When using polystyrene (PS) particles as a template,[26] GO nanosheets masked by PS particles actually exhibited electrostatic interactions with PS chains. When GO nanosheets adsorbed on PS particles were reacted with poly(2-(dimethylamino)ethyl methacrylate)(PDMAEMA), the outer surfaces of the GO nanosheets were modified using PDMAEMA by a π–π interaction, which was formed between the GO surface and the methacrylate group of PDMAEMA. Finally, PS particles were removed by treatment with a THF/water mixture, and graphene-based Janus nanosheets bearing PS chains on one side and PDMAEMA chains on the other were obtained. This preparation method was highly efficient, since PS worked as a template for masking of GO nanosheets and as a surface modifier.

Graphene-based Janus nanosheets can also be prepared using a covalent-bonding surface modifier.[27] GO nanosheets with acryloyl groups on both sides[70] were used for the formation of a Pickering emulsion in a toluene–water system. The outer surfaces of the GO nanosheets were modified through a thiol–ene reaction using PS with terminal thiol groups.[71] The GO nanosheets obtained possessed acryloyl groups on one side and PS chains on the other side. In a difference from the above-mentioned studies, the surface modifier was strongly connected to the GO surface by covalent bonds.

These PS chains were immobilized by the "grafting to" method. de Leon *et al.* prepared graphene-based Janus nanosheets bearing PMMA chains on one side by the "grafting from" method.[28] Single-layered GO nanosheets dispersed in water were modified with 2-bromoisobutyryl bromide (BIBB), which is an initiator of atom transfer radical polymerization (ATRP). A methyl methacrylate monomer was polymerized from the initiator groups. The resultant product had PMMA chains on both sides of graphene nanosheets.[72] When the

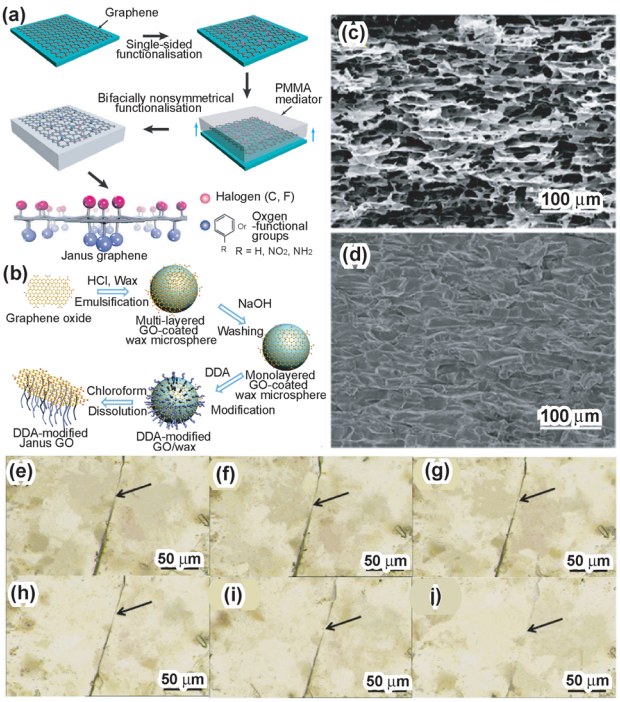

Fig. 3 (a) Scheme of the preparation of graphene-based Janus nanosheets using surface modification by a dry process. Single-sided functionalized graphene nanosheets were covered with a PMMA film and then peeled off from the substrate. The unmodified graphene surfaces were exposed and modified. Graphene-based Janus nanosheets were then obtained by PMMA removal.[24] Adapted with permission from ref. 24. Copyright 2013 Springer Nature. (b) Scheme of the preparation of graphene-based Janus nanosheets using a Pickering emulsion template.[25] Adapted with permission from ref. 25. Copyright 2015 Elsevier. (c) Cross-sectional images of graphene-based Janus nanosheet scaffolds. (d) Cross-sectional images of a graphene-based Janus nanosheet nanocomposite[80] Adapted with permission from ref. 80. Copyright 2020 American Chemical Society. A scratch was cut in a self-healing hydrogel containing graphene-based Janus nanosheets with a knife. Afterwards, the scratch was recorded for the observation of the self-healing process at (e) 0 min, (f) 5 min, (g) 10 min, (h) 15 min, (i) 20 min, and (j) 30 min, respectively.[83] Adapted with permission from ref. 83. Copyright 2020 Elsevier.

Open Access Article. Published on 23 2022. Downloaded on 08.12.2025 15:29:53.
This article is licensed under a Creative Commons Attribution-NonCommercial 3.0 Unported Licence.

same reaction was conducted on the outer surface of oil droplets in a Pickering emulsion prepared from a GO aqueous dispersion and wax, Janus nanosheets bearing PMMA chains on one side were prepared. In this study, the product's Janus structure was confirmed by AFM observation and ToF-SIMS. In the AFM images, the thickness of nanosheets bearing PMMA chains on both sides of a nanosheet was 20 nm. On the other hand, the thickness of Janus nanosheets bearing PMMA chains on only one surface was 10 nm. The ToF-SIMS results, meanwhile, demonstrated that fragments assignable to GO, m/z = 25 (C_2H^+), were observed in both nanosheets bearing PMMA chains on both surfaces and nanosheets bearing PMMA chains on only one surface. Also, fragments assignable to the ATRP initiation group, m/z = 79 and 81 (Br^+), and those assignable to PMMA chains, m/z = 31 (CH_3O^+), were observed in the MS spectrum of nanosheets bearing PMMA chains on both surfaces. In nanosheets bearing PMMA chains on only one surface, fragments assignable to PMMA chains were observed when surfaces bearing PMMA chains were exposed. On the other hand, no fragments assignable to PMMA chains were observed when surfaces bearing PMMA chains were not exposed. The contact angles of PMMA-modified surfaces with water and those of unmodified surfaces with water were different; the contact angles of PMMA-modified surfaces and unmodified surfaces with water were 61° ± 1° and 16° ± 1°, respectively. These results indicate the successful preparation of graphene-based Janus nanosheets.

Preparation of graphene-based Janus nanosheets using a liquid–liquid interface reaction was performed not only in a Pickering emulsion, but also at the interface of a biphasic system which was not emulsified.[29] A biphasic system was prepared using chloroform dissolving oleylamine and water dissolving diethanolamine. GO nanosheets with 3,4 dihydroxybenzaldehyde immobilized on both their sides were added to the aqueous phase. This reaction system was then aged for 5 days for the modification of GO at the interface. The GO surface facing an oil phase was modified with oleylamine and that facing an aqueous phase was modified with dietanolamine.

A preparation method for graphene-based Janus nanosheets with high productivity was reported.[31] First, GO nanosheets were adsorbed on template starch particles by hydrogen bonds. The outer surface of the GO nanosheets was modified with alkylamine. Finally, graphene-based Janus nanosheets were obtained by desorption of GO nanosheets from starch particles using ultrasonication and heat treatment. In this method, it was not necessary to dissolve the template particles and use a large amount of organic solvent.

There were several studies on application of amphiphilic graphene-based Janus nanosheets for oil recovery.[73–76] Graphene-based Janus nanosheets bearing an octadecylamine moiety on one side were prepared and their efficiency in oil recovery was investigated.[73] When their oil recovery performance was evaluated using rock cores, the Janus nanosheet dispersion exhibited an oil recovery factor higher than brine by 7.5%.

Graphene-based Janus nanosheets were also applied in the biological field, as drug delivery systems (DDS) and glucose sensors,[77,78] for example. Graphene-based Janus nanosheets with one hydrophilic were investigated for application in DDS.[77] The Janus nanosheets formed double-layered superstructures with two unmodified hydrophilic surfaces exposed to water. Making use of this property, an anticancer drug, camptothecin (CPT), which cannot be dissolved in water, was inserted between two Janus nanosheets in double-layered superstructures by a π–π interaction. The inserted CPT was gradually released from the double-layered superstructures into water, a characteristic property of graphene-based Janus nanosheets whose surface can bind organic targets by π–π interactions.

Graphene-based Janus nanosheets were also used for improving film properties.[79–82] Amphiphilic graphene-based Janus nanosheets increased the hydrophobicity of polymer membranes prepared *via* phase inversion. In the phase inversion process, the hydrophobic surface of the Janus nanosheets faced a porous membrane surface and the hydrophilic surface faced the liquid, leading to the change of the hydrophobic polymeric membrane surface to hydrophilic.[79] Moreover, an amphiphilic Janus nanosheet scaffold was prepared by bidirectional freeze-casting of a Janus nanosheet aqueous dispersion using ice as a template (Fig. 3c).[80] A Janus nanosheet–epoxy composite was prepared by infiltration of epoxy resin into the Janus nanosheet scaffold (Fig. 3d). The composite exhibited high in-plane thermal conductivity (~5.6 W m^{-1} K^{-1}) and high resistivity (>1014 Ω cm).

Graphene-based Janus nanosheets were also added to self-healing hydrogels, in a manner similar to that used in the study using silica-based Janus nanosheets.[83] Graphene-based Janus nanosheets bearing a poly(2-(acryloyloxy)ethyl ferrocenecarboxylate) (PMAEFc) moiety on one side and polydopamine (PDA) on the other side of individual nanosheets and $FeCl_3 \cdot 6H_2O$ were added to a poly(acrylic acid) (PAA) hydrogel containing poly(acryloyl-β-cyclodextrin) (PACD) chains. The self-healing efficiency was improved by metal–ligand coordination between Fe(III) ions in the hydrogel and the catechol moiety on the Janus nanosheets and a host–guest interaction between the ferrocene moiety in the Janus nanosheets and β-cyclodextrin in the hydrogel (Fig. 3e–j). The mechanical strength was also increased compared with that of PAA.

Yuan *et al.* prepared graphene-based Janus nanosheets using two surface modifiers for the modification of both sides of nanosheets and successfully adsorbed several types of inorganic and organic targets.[30] Silica particles modified with APTES were used as a template. Single-layered GO nanosheets were adsorbed onto the silica particles, and the outer surface of the GO nanosheets was modified using ethylenediamine tetraacetic acid (EDTA). The products were treated with KOH to remove the silica particles. The unmodified surface of the GO nanosheets was then modified using octadecylamine. This product adsorbed inorganic targets, such as Pb(II) and Ni(II) ions, and an organic target, perfluorooctanesulfonic acid (PFOS), on the surfaces bearing the EDTA group and octadecylamine group, respectively.

 This journal is © The Royal Society of Chemistry 2022

Open Access Article. Published on 23 2022. Downloaded on 08.12.2025 15:29:53.
This article is licensed under a Creative Commons Attribution-NonCommercial 3.0 Unported Licence.

Janus nanosheets based on clay minerals and ion-exchangeable layered materials

Other than graphite, there are various types of layered materials consisting of charged nanosheets, such as clay minerals and layered transition metal oxides. Some of these layered materials can accommodate ionic species charged oppositely to the layer charge, typically metal ions in interlayer spaces. Exfoliated nanosheets can also be modified by electrostatic interactions. Moreover, surface modification that forms covalent bonds between nanosheet surfaces and modifiers can be achieved using an alcohol, a silane coupling agent or a phosphorus-containing coupling agent.[84] These modification methods have been used for the preparation of Janus nanosheets.

There have been a few reports on the preparation of clay-based Janus nanosheets.[33–35] Some clay minerals have layered structures with nanosheets stacked in a way similar to graphite. These nanosheets typically consist of SiO_4 tetrahedra and AlO_6 octahedra and are stacked with interlayer cations in many layered clay minerals, some of which are exchangeable with other cations.[85] These layered clay minerals with an ion-exchange capability can be swollen and exfoliated in water due to their low layer charge density to provide exfoliated clay nanosheets.[86] Clay-based Janus nanosheets were prepared by regioselective surface modification of the clay nanosheets. There were a large number of reports on the functionalization of clay nanosheet surfaces. Interlayer cations could be exchanged with positively charged species, including metal cations, organoammonium ions and cationic dyes.[87] Moreover, the surfaces of clay nanosheets with aluminol surfaces, such as kaolinite, could be modified with silane coupling agents and alcohols.[88,89] Thus, a large number of inorganic–organic materials have been prepared.

Liu *et al.* prepared LAPONITE®-based Janus nanosheets.[33] LAPONITE®, a synthetic hectorite clay mineral, consists of negatively charged nanosheets and interlayer cations. First, PS particles were added to a single-layered LAPONITE® nanosheet aqueous dispersion. LAPONITE® nanosheets were adsorbed on the PS particle surfaces by an electrostatic interaction between the positively charged PS particles and the negatively charged LAPONITE® nanosheets. The PS particles were then dissolved in THF. As a result, LAPONITE®-based Janus nanosheets bearing PS chains on one side were prepared. This preparation method was similar to that used for the preparation of graphene-based Janus nanosheets.[27] Furthermore, the unmodified surface of the Janus nanosheets was reacted with PDMAEMA. The Janus nanosheets obtained had PS chains on one side and PDMAEMA chains on the other side of individual LAPONITE® nanosheets.

Janus nanosheets can also be prepared by controlled exfoliation of fluorohectorite, a clay mineral with interlayer Na^+.[34] Fluorohectorite in which an Na^+ interlayer and an NH_4^+ interlayer appeared alternately was prepared by a controlled ion-exchange reaction of interlayer Na^+ with NH_4^+. Since the interlayer charge densities of the Na^+ site and NH_4^+ site were different from each other, the exfoliation behavior of these two interlayers were also different.[90,91] Fluorohectorite-based Janus nanosheets were prepared using these reactivity differences. First, fluorohectorite with alternating Na^+ and NH_4^+ interlayers was prepared, and the Na^+ interlayer was exfoliated in water. Both outer surfaces of the individual double-layered nanosheets obtained were then modified with one type of cationic polymer. In this process, the unexfoliated surfaces were masked from surface modification. The NH_4^+ interlayer of the product was then exfoliated under basic conditions, such as in a LiOH aqueous solution. The unmodified surface of the single-layered nanosheets obtained was then modified using the other cationic polymer (Fig. 4a).

Kaolinite and halloysite are clay minerals consisting of neutral and compositionally asymmetric nanosheets with one surface covered with aluminol and the other consisting of a Si–O network. The aluminol surface and silica surface exhibit different reactivities toward several types of surface modifiers. Therefore, regioselective surface modification can be achieved.[92–96] In methoxy-modified kaolinite whose aluminol surface was regioselective and partially modified with methanol, the aluminol surface was further modified with a mixture of APTES and trimethoxyvinylsilane.[97] This organically modified kaolinite consisted of stacked Janus nanosheets bearing both an APTES moiety and a vinyl moiety on one side. A polymer composite with kaolinite-based Janus nanosheets was

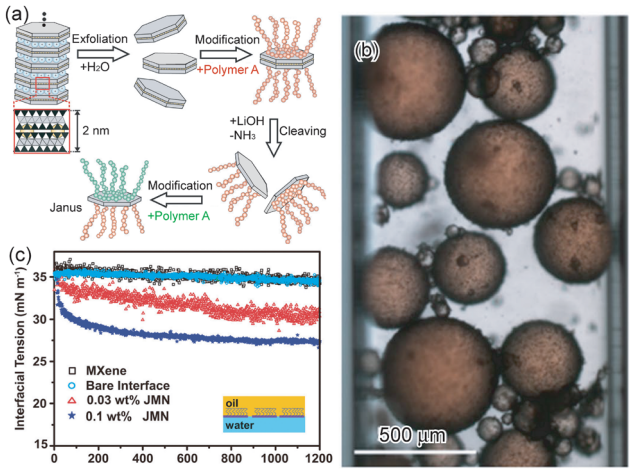

Fig. 4 (a) Scheme of the preparation of fluorohectorite-based Janus nanosheets. The yellow and blue colored circles are NH_4^+ and hydrated Na^+, respectively. After selective exfoliation of the Na^+ layer, the exposed surface was modified using polymer A. The NH^{4+} layer was then exfoliated, and the unmodified surface was modified with polymer B.[34] Adapted with permission from ref. 34. Copyright 2016 John Wiley and Sons. (b) Optical microscopy image of an O/W emulsion: the emulsion is stabilized by halloysite-based Janus nanosheets. The oil phase is dodecane colored with Sudan IV red.[35] Adapted with permission from ref. 35. Copyright 2019 Springer Nature. (c) The dynamic interfacial tension of the water–toluene interface under different conditions; the MXene-based Janus nanosheets contents are 0.03 wt% and 0.1 wt%.[110] Adapted with permission from ref. 110. Copyright 2020 Chinese Chemical Society (CCS), Institute of Chemistry of Chinese Academy of Sciences (IC), and the Royal Society of Chemistry.

Open Access Article. Published on 23 2022. Downloaded on 08.12.2025 15:29:53.
This article is licensed under a Creative Commons Attribution-NonCommercial 3.0 Unported Licence.

obtained by polymerization of styrene involving an immobilized vinyl moiety. This composite formed a vesicle in water by self-assembly. Halloysite-based Janus nanosheets were also prepared.[35] First, their aluminol surface was modified using phenylphosphonic acid to form a hydrophobic surface. Then, ATRP initiator groups were introduced to the silica surface and PDMAEMA chains were grown from the ATRP initiator groups to form a hydrophilic surface.

Preparation of layered transition metal oxide-based Janus nanosheets was also achieved using a layered hexaniobate, $K_4Nb_6O_{17}{\cdot}3H_2O$. $K_4Nb_6O_{17}{\cdot}3H_2O$ consists of stacked $[Nb_6O_{17}]^{4-}$ nanosheets and exchangeable interlayer K^+, with interlayer I with high reactivity and interlayer II with low reactivity appearing alternately.[98] There were studies on the regioselective exchange of interlayer K^+ and modification of the interlayer surface.[99,100] We have successfully prepared $K_4Nb_6O_{17}{\cdot}3H_2O$-based Janus nanosheets utilizing this unique reactivity difference. The surfaces of interlayers I and II were modified using phosphorus-containing coupling agents, which have the advantages of stability of the formed Nb–O–P bonds toward hydrolysis and suppression of multi-layer formation *via* homocondensation under mild reaction conditions.[101,102] Therefore, interlayers I and II were regioselectively modified by stepwise reactions. Since the surfaces of interlayers I and II did not react directly with phosphorus-containing coupling agents, the interlayer I surface was modified using a phosphorus-containing coupling agent after expanding interlayer I by introduction of bulky dioctadecyldimetylammonium ions. $K_4Nb_6O_{17}{\cdot}3H_2O$-based Janus nanosheets bearing a phosphorus-containing coupling agent moiety on one side and an unmodified surface were obtained by exfoliation of the product. By using this method, $K_4Nb_6O_{17}{\cdot}3H_2O$-based Janus nanosheets bearing PNIPAAm chains and an ion-exchangeable unmodified surface were prepared.[103] When the interlayer II surface was further modified without an exfoliation procedure at interlayer II using the other phosphorus-containing coupling agent after expanding interlayer II by the introduction of dodecylammonium ions, $K_4Nb_6O_{17}{\cdot}3H_2O$-based Janus nanosheets in which two types of moieties were regioselectively immobilized on the two sides of the individual nanosheets were obtained; Janus nanosheets bearing an octadecyl moiety on one side and a carboxypropyl moiety on the other were reported.[104] This study confirmed the Janus structure of this type of nanosheets based on AFM observation. For the AFM observation, nanosheets were immobilized on Si wafers by casting a Janus nanosheet dispersion and subsequent drying. In the topo image, nanosheets with similar thickness values were observed. In the phase image of the same area, on the other hand, these nanosheets exhibited two types of phases. These results indicate that the nanosheets had different properties on the two types of surfaces. It was therefore confirmed that $K_4Nb_6O_{17}{\cdot}3H_2O$-based Janus nanosheets were successfully prepared *via* regioselective surface modification and exfoliation.

MXenes, which were first reported in 2011, comprise two-dimensional transition metal carbides and nitrides obtained from MAX phases.[105] The composition of MXenes can be represented as $M_{n+1}X_nT_x$ (M: transition metal, X: carbon or nitrogen and T: surface group, OH, O and F). As with clay minerals and $K_4Nb_6O_{17}{\cdot}3H_2O$, there were reports on the intercalation of metal ions into MXenes[106,107] as well as surface modification.[108,109] Zhao *et al.* prepared MXene-based Janus nanosheets.[110] $Ti_3C_2T_x$ MXenes were exfoliated in water using ultrasonication treatment. MXene nanosheets, which had a negative charge, were adsorbed on PS particles by electrostatic interactions. After removing the PS particles, MXene-based Janus nanosheets bearing PS chains on one side were obtained by dissolving the excess PS.

These Janus nanosheets can be applied as two-dimensional surfactants. LAPONITE®-based Janus nanosheets bearing PS chains and PDMAEMA chains were used as an emulsifier for toluene and water.[33] The assembly structure of this type of Janus nanosheet in THF–methanol was also examined. Since PS has no affinity toward methanol while PDMAEMA has a good affinity toward it, double-layered structures possibly formed when Janus nanosheet surfaces bearing PS chains faced each other. Since the above-mentioned halloysite-based Janus nanosheets had both a hydrophobic surface and a hydrophilic surface on their two sides,[35] these Janus nanosheets have performed as a two-dimensional surfactant for cases such as stabilization of emulsions and decreasing the dodecane–water interface (Fig. 4b).

MXene-based Janus nanosheets were also applied as a surfactant.[110] The interface tension between water and toluene was gradually decreased by adding Janus nanosheets for 20 min, indicating that Janus nanosheets took 20 min to assemble at the water–oil interface (Fig. 4c). This water–toluene emulsion containing Janus nanosheets was also freeze-dried, and aerogels consisting of MXene-based Janus nanosheets were prepared. This aerogel had a low bulk density, which was tunable by changing the concentration of Janus nanosheets.

$K_4Nb_6O_{17}{\cdot}3H_2O$-based Janus nanosheets with surface activity were also reported.[111] Janus nanosheets bearing a hydrophilic dihydroxyphosphonate moiety and a hydrophobic phenylphosphonic moiety showed a slower decrease in surface tension at an air–water interface than that achieved with molecular surfactants. In an emulsion of toluene and aqueous Janus dispersion, unique coalescence and Ostwald ripening behaviour was also observed. It was reported that, in O/W emulsions containing molecular surfactants, oil droplets coalesced and immediately changed their shapes to form perfect spheres.[112] A similar phenomenon was observed in an O/W emulsion containing Janus nanosheets. Oil droplets immersed with the Janus nanosheets coalesced, resulting in ellipsoidal droplets which were further changed to spherical droplets. The Ostwald ripening rate of oil droplets in the emulsion containing Janus nanosheets (1.2×10^{-20} m^3 s^{-1}) was larger than that of a molecular surfactant (9.2×10^{-22} m^3 s^{-1})[113] due to the heavy weight and bulky sheet-like shape of the Janus nanosheets.

Summary and outlook

Currently, many different types of inorganic material-based Janus nanosheets with different compositions and surface pro-

 This journal is © The Royal Society of Chemistry 2022

Open Access Article. Published on 23 2022. Downloaded on 08.12.2025 15:29:53.
This article is licensed under a Creative Commons Attribution-NonCommercial 3.0 Unported Licence.

perties have been designed for the exploration of their properties and applications. This review summarizes several types of inorganic material-based Janus nanosheets prepared from various molecular inorganic precursors and layered materials using their characteristic properties and reactivities.

Silica-based Janus nanosheets have been extensively studied using two-dimensional sol–gel reactions of alkoxysilanes as inorganic precursors. In this process, regioselective functionalization is achieved by self-assembly of organoalkoxysilanes and post-treatment of the surface modifications typically using organoalkoxysilanes. Preparation of graphene-based Janus nanosheets is also achieved by regioselective functionalization and/or surface modification of graphene nanosheets prepared by exfoliation of graphite. Other than clay minerals, $K_4Nb_6O_{17}{\cdot}3H_2O$ and MXenes, which consist of nanosheets different from the above graphene nanosheets from the viewpoints of chemical composition and exfoliation behavior, can also be used as the starting inorganic materials, and their Janus nanosheets can be prepared by using the characteristic reactivities of their interlayer and/or layer surfaces. In most cases, functional surface modifiers are bound on the nanosheet surfaces *via* bonds and interactions including covalent bonds, electrostatic interactions, π–π interactions. The Janus nanosheets obtained were not always dispersed as single-layered nanosheets which expose two different surfaces. The results showed that Janus nanosheets with relatively hydrophilic surface functional groups on both sides can be initially dispersed as single-layered nanosheets, but then form aggregates after standing for a few months.[111] It was also reported that the structures of graphene-based Janus nanosheets were converted into double-layered structures with a hydrophobic internal space and hydrophilic external surfaces in water.[77] The dispersibility of Janus nanosheets bearing two types of stimuli-responsive polymers on two surfaces could be controlled, moreover, by two types of stimuli, such as changing temperature and pH.[44]

The Janus nanosheets themselves are expected to show two distinct characteristics comprising different hydrophilicities/hydrophobicities and different stimuli responses. As mentioned above, the Janus nanosheets with different hydrophilicity/hydrophobicity properties are particularly interesting, because they can be considered as "giant" surfactants which can stabilize droplets in binary oil/water systems. By reducing the lateral size of the nanosheets and the size of the droplets (as porogens) through application of a strong homogenizer, *etc*., much smaller pores on the nanometer scale can be synthesized. It is also expected that one surface of the Janus nanosheets, which should be ideal for target applications, can be exposed within the pores in a controlled manner. This is the real uniqueness of using Janus nanosheets. In addition, very thin Janus nanosheets can be directly dispersed in a matrix (*e.g.*, hydrogels, polymers) to create new types of composite materials. Recently, many technologies using electric[114] and magnetic[115] fields have been developed for precise control of the alignment of nanosheets in a matrix. When Janus nanosheets can be aligned well, we can expect unique anisotropic properties, in which different properties are observed on different faces of the matrix, a result which is not attainable with traditional Janus "nanoparticles" and "nanosheets".

By using different kinds of Janus nanosheets with organic surface modification as building blocks, various inorganic heterojunction structures can be synthesized in a designed manner. These Janus nanosheets can be chemically connected to each other through covalent or non-covalent interactions (*e.g.*, electrostatic interactions, hydrogen-bonding, host–guest interactions, *etc*.). Such programmed assembly avoids thermodynamically stable states, thereby bringing out unexpected properties. Further removal of organic components by the calcination or extraction method can create highly functional heterojunctions of inorganic nanomaterials with atomic-scale precision. Sometimes, the organic components can be intentionally retained and further converted to carbons by applying low-temperature calcination. The presence of inter-nanosheeet carbon would be useful for the enhancement of the whole conductivity of hybrid materials and provide additional positive effects in terms of performance. Thus, artificially designed hybrid materials are highly attractive for a wide range of applications because of the modified electronic properties and new physical or chemical properties arising from the combination of two or more materials.

For instance, a metal/semiconductor interface is promising as a structure for better harvesting hot carriers *via* the transfer of hot electrons generated on a metal into a semiconductor and then for achieving higher charge separation and catalytic efficiency. If synthetic methodologies are developed in the future, multi-interface systems composed of different kinds of metals and semiconductors, such as Au/rutile/anatase and mesoporous $Au/CdS/TiO_2/WO_3$, will also be artificially designed by manipulating the conduction band (CB) potential of individual semiconductor layers. Such multi-interface systems could exhibit higher catalytic efficiency, far exceeding that of double-interface systems using conventional Janus nanosheets with two properties, as a result of the consecutive transfer of hot electrons that are finally consumed in chemical reactions.

As an additional attribute to be explored, we should take full advantage of the unique capabilities of porous structures, which can be prepared *via* the use of interactions between inorganic species and micelles. Although this strategy has been extended from silica[116–118] to various metal oxides[119] and metals,[120] only silica-based Janus nanosheets with a porous sheet structure have been achieved.[22] It will therefore be possible to introduce meso/nanoporous architectures in each layer of inorganic Janus nanosheets with different metal oxide and metal compositions. This technology will allow us to not only modulate the transport of phonons and thermal energy, but also to enhance various chemical reactions using porous inorganic Janus nanosheets as has been shown for aqueous hydrogenation reactions.[22] These research efforts are oriented toward the aim of developing functions that cannot be achieved with conventional Janus "nanoparticles" and "nanosheets".

Open Access Article. Published on 23 2022. Downloaded on 08.12.2025 15:29:53.
This article is licensed under a Creative Commons Attribution-NonCommercial 3.0 Unported Licence.

Conflicts of interest

There are no conflicts to declare.

Acknowledgements

This work was financially supported in part by the JST-ERATO Yamauchi Materials Space-Tectonics Project (JPMJER2003).

References

1 H. Dong, L. Wu, L. Zhang, H. Chen and C. Gao, *J. Membr. Sci.*, 2015, **494**, 92–103.
2 M. Osada and T. Sasaki, *J. Mater. Chem.*, 2009, **19**, 2503–2511.
3 S. J. Clarke, P. Adamson, S. J. C. Herkelrath, O. J. Rutt, D. R. Parker, M. J. Pitcher and C. F. Smura, *Inorg. Chem.*, 2008, **47**, 8473–8486.
4 P. Liu, *Appl. Clay Sci.*, 2007, **38**, 64–76.
5 A. B. Bourlinos, D. Gournis, D. Petridis, T. Szabó, A. Szeri and I. Dékány, *Langmuir*, 2003, **19**, 6050–6055.
6 C. Tirayaphanitchku, K. Imwiset and M. Ogawa, *Bull. Chem. Soc. Jpn.*, 2021, **94**, 678–693.
7 Y. Mitamura, Y. Komori, S. Hayashi, Y. Sugahara and K. Kuroda, *Chem. Mater.*, 2001, **13**, 3747–3753.
8 A. Shimada, Y. Yoneyama, S. Tahara, P. H. Mutin and Y. Sugahara, *Chem. Mater.*, 2009, **21**, 4155–4162.
9 N. Liu, F. Luo, H. Wu, Y. Lui, C. Zhang and J. Chen, *Adv. Funct. Mater.*, 2008, **18**, 1518–1525.
10 N. H. Kim, S. V. Malhota and M. Xanthos, *Microporous Mesoporous Mater.*, 2006, **96**, 29–35.
11 M. Zhang, Y. Li, Z. Su and G. Wei, *Polym. Chem.*, 2015, **6**, 6107–6124.
12 P. G. de Gennes, *Angew. Chem., Int. Ed. Engl.*, 1992, **31**, 842–845.
13 M. Lattuada and T. A. Hatton, *Nano Today*, 2011, **6**, 286–308.
14 L. Zhang, Z. Yang, T. Gong, R. Pan, H. Wang, Z. Guo, H. Zhang and X. Fu, *J. Mater. Chem. A.*, 2020, **8**, 8813–8830.
15 Y. Duan, X. Zhao, M. Sun and H. Hao, *Ind. Eng. Chem. Res.*, 2021, **60**, 1071–1095.
16 F. Liang, K. Shen, X. Qu, C. Zhang, Q. Wang, J. Li, J. Liu and Z. Yang, *Angew. Chem., Int. Ed.*, 2011, **50**, 2379–2382.
17 J. Zhang, S. Jia, I. Kholmanov, L. Dong, D. Er, W. Chen, H. Guo, Z. Jin, V. B. Shenoy, L. Shi and J. Lou, *ACS Nano*, 2017, **11**, 8192–8198.
18 R. Li, Y. Cheng and W. Huang, *Small*, 2018, **14**, 1802091.
19 K. Lee, M. D. Losego, D. H. Kim and G. N. Parsons, *Mater. Horiz.*, 2014, **1**, 419–423.
20 Y. Liu, F. Liang, Q. Wang, X. Qu and Z. Yang, *Chem. Commun.*, 2015, **51**, 3562–3565.
21 D. Xue, X. Song and F. Liang, *RSC Adv.*, 2017, **7**, 25450–25454.
22 S. Yan, H. Zou, S. Chen, N. Xue and H. Yang, *Chem. Commun.*, 2018, **54**, 10455–10458.
23 T. Yin, Z. Yang, M. Lin, J. Zhang and Z. Dong, *Chem. Eng. J.*, 2019, **371**, 507–515.
24 L. Zhang, J. Yu, M. Yang, Q. Xie, H. Peng and Z. Liu, *Nat. Commun.*, 2013, **4**, 1443.
25 H. Wu, W. Yi, Z. Chen, H. Wang and Q. Du, *Carbon*, 2015, **93**, 473–483.
26 Y. Yang, L. Zhang, X. Ji, L. Zhang, H. Wang and H. Zhao, *Macromol. Rapid Commun.*, 2016, **37**, 1520–1526.
27 B. T. McGrail, J. D. Mangadlao, B. J. Rodier, J. Swisher, R. Advincula and E. Pentzer, *Chem. Commun.*, 2016, **52**, 288–291.
28 A. C. de Leon, B. J. Rodier, Q. Luo, C. M. Hemmingsen, P. Wei, K. Abbasi, R. Advincula and E. B. Pentzer, *ACS Nano*, 2017, **11**, 7485–7493.
29 S. Georgitsopoulou, A. Karakassides and V. Georgakilas, *Chem. Eur. J.*, 2018, **24**, 17356–17360.
30 K. Yuan, Y. Li, X. Huang, Y. Liang, Q. Liu and G. Jiang, *Chem. Commun.*, 2019, **55**, 4957–4960.
31 D. Luo, F. Wang, B. V. Vu, J. Chen, J. Bao, D. Cai, R. C. Willson and Z. Ren, *Carbon*, 2018, **126**, 105–110.
32 A. Kouloumpis, D. D. Chronopoulos, G. Potsi, M. Pykal, J. Vlček, M. Scheibe and M. Otyepka, *Chem. – Eur. J.*, 2020, **26**, 6518–6524.
33 J. Liu, G. Liu, M. Zhang, P. Sun and H. Zhao, *Macromolecules*, 2013, **46**, 5974–5984.
34 M. Stöter, S. Gödrich, P. Feicht, S. Rosenfeldt, H. Thurn, J. W. Neubauer, M. Seuss, P. Lindner, H. Kalo, M. Möller, A. Fery, S. Förster, G. Papastavrou and J. Breu, *Angew. Chem., Int. Ed.*, 2016, **55**, 7398–7402.
35 L. Zhang, Q. Lei, J. Luo, M. Zeng, L. Wang, D. Huang, X. Wang, S. Mannan, B. Peng and Z. Cheng, *Sci. Rep.*, 2019, **9**, 163.
36 S. P. Mukherjee, *J. Non-Cryst. Solids*, 1980, **42**, 477–488.
37 S.-S. Choi, S. G. Lee, S. S. Im, S. H. Kim and Y. L. Joo, *J. Mater. Sci. Lett.*, 2003, **22**, 891–893.
38 C. J. Brinker, A. J. Hurd, G. C. Frye, K. J. Ward and C. S. Ashley, *J. Non-Cryst. Solids*, 1990, **121**, 294–302.
39 L. P. Singh, S. K. Bhattacharyya, R. Kumar, G. Mishra, U. Sharma, G. Singh and S. Ahalawat, *Adv. Colloid Interface Sci.*, 2014, **214**, 17–37.
40 Z. A. ALOthman, *Materials*, 2012, **5**, 2874–2902.
41 D. Gnanasekaran, K. Madhavan and B. S. R. Reddy, *J. Sci. Ind. Res.*, 2009, **68**, 437–464.
42 L. L. Hench and J. K. West, *Chem. Rev.*, 1990, **90**, 33–72.
43 Y. Chen, F. Liang, H. Yang, C. Zhang, Q. Wang, X. Qu, J. Li, Y. Cai, D. Qiu and Z. Yang, *Macromolecules*, 2012, **45**, 1460–1467.
44 H. Yang, F. Liang, X. Wang, Y. Chen, C. Zhang, Q. Wang, X. Qu, J. Li, D. Wu and Z. Yang, *Macromolecules*, 2013, **46**, 2754–2759.
45 Z. Zhao, F. Liang, G. Zhang, X. Ji, Q. Wang, X. Qu, X. Song and Z. Yang, *Macromolecules*, 2015, **48**, 3598–3603.
46 Z. Cao, G. Wang, Y. Chen, F. Liang and Z. Yang, *Macromolecules*, 2015, **48**, 7256–7261.

 This journal is © The Royal Society of Chemistry 2022

Open Access Article. Published on 23 2022. Downloaded on 08.12.2025 15:29:53.
This article is licensed under a Creative Commons Attribution-NonCommercial 3.0 Unported Licence.

47 T. Yin, Z. Yang, Z. Dong, M. Lin and J. Zhang, *Fuel*, 2019, **237**, 344–351.
48 X. Ji, Q. Zhang, F. Liang, Q. Chen, X. Qu, C. Zhang, Q. Wang, J. Li, X. Song and Z. Yang, *Chem. Commun.*, 2014, **50**, 5706–5709.
49 Q. B. Meng, P. Yang, T. Feng, X. Ji, Q. Zhang, D. Liu, S. Wu, F. Liang, Z. Zheng and X. Song, *J. Colloid Interface Sci.*, 2017, **507**, 74–82.
50 X. Zhang, H. Ren and A. He, *Nanoscale*, 2018, **10**, 19351–19359.
51 T. Yin, Z. Yang, F. Zhang, M. Lin, J. Zhang and Z. Dong, *J. Colloid Interface Sci.*, 2021, **583**, 214–221.
52 T. Yin, Z. Yang, M. Lin, J. Zhang and Z. Dong, *Ind. Eng. Chem. Res.*, 2019, **58**, 4479–4486.
53 X. Ji, Q. Zhang, X. Qu, Q. Wang, X. Song, F. Liang and Z. Yang, *RSC Adv.*, 2015, **5**, 21877–21880.
54 J. Yang, X. Xu, Y. Liu, Y. Gao, H. Chen and H. Li, *Colloids Surf., A*, 2019, **582**, 123858.
55 X. Xu, Y. Liu, Y. Gao and H. Li, *Colloids Surf., A*, 2017, **529**, 613–620.
56 A. Kirillova, C. Schliebe, G. Stoychev, A. Jakob, H. Lang and A. Synytska, *ACS Appl. Mater. Interfaces*, 2015, **7**, 21218–21225.
57 L. Xia, H. Zhang, Z. Wei, Y. Jiang, L. Zhang, J. Zhao, J. Zhang, L. Dong, E. Li, L. Ruhlmann and Q. Zhang, *Chem. – Eur. J.*, 2017, **23**, 1920–1929.
58 D. Xue, Q. B. Meng and X. Song, *ACS Appl. Mater. Interfaces*, 2019, **11**, 10967–10974.
59 C. Li, S. Liu, Y. Pi, J. Feng, Z. Liu, S. Li and R. Tan, *J. Catal.*, 2021, **395**, 236–245.
60 J. Yang, J. Wang, Y. Liu, H. Lia and Z. Lin, *Mater. Horiz.*, 2020, **7**, 3242–3249.
61 C. Li, Y. Pi, S. Liu, J. Feng, X. Zhang, S. Li and R. Tan, *ACS Sustainable Chem. Eng.*, 2021, **9**, 13501–13513.
62 H. Nie, X. Liang and A. He, *Macromolecules*, 2018, **51**, 2615–2620.
63 X. Han, X. Liang, L. Cai, A. He and H. Nie, *Polym. Chem.*, 2019, **10**, 5184–5190.
64 Y. Hou, G. Zhang, X. Tang, Y. Si, X. Song, F. Liang and Z. Yang, *Macromolecules*, 2019, **52**, 3863–3868.
65 Z. Xu, J. Lin, J. Chen, J. Lin and Q. Chen, *Polym. Test.*, 2021, **98**, 107159.
66 M. Li, X. Li, C. Li, H. Liu, W. Wang, L. Bai, H. Chen and L. Yang, *Eur. Polym. J.*, 2021, **155**, 110580.
67 W. S. Hummers and R. E. Offeman, *J. Am. Chem. Soc.*, 1958, **80**, 1339.
68 Y. Zhu, S. Murali, W. Cai, X. Li, J. W. Suk, J. R. Potts and R. S. Ruoff, *Adv. Mater.*, 2010, **22**, 3906–3924.
69 J. Liu, L. Cui and D. Losic, *Acta Biomater.*, 2013, **9**, 9243–9257.
70 B. T. McGrail, B. J. Rodier and E. Pentzer, *Chem. Mater.*, 2014, **26**, 5806–5811.
71 Y. He, F. Wu, X. Sun, R. Li, Y. Guo, C. Li, L. Zhang, F. Xing, W. Wang and J. Gao, *ACS Appl. Mater. Interfaces*, 2013, **5**, 4843–4855.
72 G. Gonçalves, P. A. A. P. Marques, A. Barros-Timmons, I. Bdkin, M. K. Singh, N. Emami and J. Grácio, *J. Mater. Chem.*, 2010, **20**, 9927–9934.
73 D. Luo, F. Wang, J. Zhu, L. Tang, Z. Zhu, J. Bao, R. C. Willson, Z. Yang and Z. Ren, *Ind. Eng. Chem. Res.*, 2017, **56**, 11125–11132.
74 D. Luo, F. Wang, M. K. Alam, F. Yu, I. K. Mishra, J. Bao, R. C. Willson and Z. Ren, *Chem. Mater.*, 2017, **29**, 3454–3460.
75 D. Luo, F. Wang, J. Chen, F. Zhang, L. Yu, D. Wang, R. C. Willson, Z. Yang and Z. Ren, *Langmuir*, 2018, **34**, 3694–3700.
76 D. Luo, F. Zhang, F. Ding, B. Ren and Z. Ren, *Soft Matter*, 2019, **15**, 7472–7478.
77 V. Bekiari, A. Karakassides, S. Georgitsopoulou, A. Kouloumpis, D. Gournis and V. Georgakilas, *J. Mater. Sci.*, 2018, **53**, 11167–11175.
78 F. Poletti, L. Favaretto, A. Kovtun, E. Treossi, F. Corticelli, M. Gazzano, V. Palermo, C. Zanardi and M. Melucci, *J. Phys. Mater.*, 2020, **3**, 014011.
79 M. Akbari, M. Shariaty-Niassar, T. Matsuura and A. F. Ismail, *J. Colloid Interface Sci.*, 2018, **527**, 10–24.
80 Y. Wang, Z. Zhang, T. Li, P. Ma, X. Zhang, B. Xia, M. Chen, M. Du, T. Liu and W. Dong, *ACS Appl. Mater. Interfaces*, 2020, **12**, 44273–44280.
81 C.-M. Kim, S. Hong, R. Li, I. S. Kim and P. Wang, *ACS Sustainable Chem. Eng.*, 2019, **7**, 7252–7259.
82 I. Jeon, M. D. Peeks, S. Savagatrup, L. Zeininger, S. Chang, G. Thomas, W. Wang and T. M. Swager, *Adv. Mater.*, 2019, **31**, 1900438.
83 A. Ma, G. Wang, Z. Yang, L. Bai, H. Chen, W. Wang, H. Yang, D. Wei and L. Yang, *Chem. Eng. J.*, 2020, **385**, 123962.
84 C. Tirayaphanitchkul, K. Imwiset and M. Ogawa, *Bull. Chem. Soc. Jpn.*, 2021, **94**, 678–693.
85 M. F. Brigatti, E. Galán and B. K. G. Theng, *Dev. Clay Sci.*, 2013, **5**, 21–81.
86 V. Nicolosi, M. Chhowalla, M. G. Kanatzidis, M. S. Strano and J. N. Coleman, *Science*, 2013, **340**, 1226419.
87 T. J. Pinnavaia, *Science*, 1983, **220**, 365–371.
88 C. Detellier, *Chem. Rec.*, 2018, **18**, 868–877.
89 H. He, Q. Tao, J. Zhu, P. Yuan, W. Shen and S. Yang, *Appl. Clay Sci.*, 2013, **71**, 15–20.
90 M. W. Möller, D. Hirsemann, F. Haarmann, J. Senker and J. Breu, *Chem. Mater.*, 2010, **22**, 186–196.
91 M. Stöter, B. Biersack, N. Reimer, M. Herling, N. Stock, R. Schobert and J. Breu, *Chem. Mater.*, 2014, **26**, 5412–5419.
92 J. L. Guimarães, P. Peralta-Zamora and F. Wypych, *J. Colloid Interface Sci.*, 1998, **206**, 281–287.
93 J. J. Tunney and C. Detellier, *J. Mater. Chem.*, 1996, **6**, 1679–1685.
94 Y. Komori, H. Enoto, R. Takenawa, S. Hayashi, Y. Sugahara and K. Kuroda, *Langmuir*, 2000, **16**, 5506–5508.

Open Access Article. Published on 23 2022. Downloaded on 08.12.2025 15:29:53.
This article is licensed under a Creative Commons Attribution-NonCommercial 3.0 Unported Licence.

95 W. O. Yah, A. Takahara and Y. M. Lvov, *J. Am. Chem. Soc.*, 2012, **134**, 1853–1859.
96 S. Machida, N. Idota and Y. Sugahara, *Dalton Trans.*, 2019, **48**, 11663–11673.
97 P. Anju and V. S. Prasad, *Langmuir*, 2020, **36**, 1761–1767.
98 K. Nassau, J. W. Shiever and J. L. Bernstein, *J. Electrochem. Soc.*, 1969, **116**, 348–353.
99 Q. Wei and T. Nakato, *Microporous Mesoporous Mater.*, 2006, **96**, 84–92.
100 N. Kimura, Y. Kato, R. Suzuki, A. Shimada, S. Tahara, T. Nakato, K. Matsukawa, P. H. Mutin and Y. Sugahara, *Langmuir*, 2014, **30**, 1169–1175.
101 G. Guerrero, J. G. Alauzun, M. Granier, D. Laurencin and P. H. Mutin, *Dalton Trans.*, 2013, **42**, 12569–12585.
102 G. Guerrero, P. H. Mutin and A. Vioux, *Chem. Mater.*, 2001, **13**, 4367–4373.
103 R. Suzuki, N. Idota, T. Nishimi and Y. Sugahara, *Chem. Lett.*, 2020, **49**, 1058–1061.
104 R. Suzuki, M. Sudo, M. Hirano, N. Idota, M. Kunitake, T. Nihimi and Y. Sugahara, *Chem. Commun.*, 2018, **54**, 5756–5759; R. Suzuki, M. Sudo, M. Hirano, N. Idota, M. Kunitake, T. Nihimi and Y. Sugahara, in *Functional Materials [On line]*, ed. E. R. Sahu, IntechOpen, London, 2019, ch. 3.
105 M. Naguib, M. Kurtoglu, V. Presser, J. Lu, J. Niu, M. Heon, L. Hultman, Y. Gogotsi and M. W. Barsoum, *Adv. Mater.*, 2011, **23**, 4248–4253.
106 N. C. Osti, M. Naguib, A. Ostadhossein, P. R. C. Kent, B. Dyatkin, G. Rother, W. T. Heller, A. C. T. van Duin, Y. Gogotsi and E. Mamontov, *ACS Appl. Mater. Interfaces*, 2016, **8**, 8859–8863.
107 H.-J. Koh, S. J. Kim, K. Maleski, S.-Y. Cho, Y.-J. Kim, C. W. Ahn, Y. Gogotsi and H.-T. Jung, *ACS Sens.*, 2019, **4**, 1365–1372.
108 H. Riazi, M. Anayee, K. Hantanasirisakul, A. A. Shamsabadi, B. Anasori, Y. Gogotsi and M. Soroush, *Adv. Mater. Interfaces*, 2020, **7**, 1902008.
109 Y. Sun, Y. Zhang, H. X. Zhang, M. Liu and Y. Liu, *Anal. Chem.*, 2020, **92**, 10668–10676.
110 S. Zhao, L. Li, H.-B. Zhang, B. Qian, J.-Q. Luo, Z. Deng, S. Shi, T. P. Russellcde and Z.-Z. Yu, *Mater. Chem. Front.*, 2020, **4**, 910–917.
111 R. Suzuki, T. Nagai, E. Onitsuka, N. Idota, M. Kunitake, T. Nishimi and Y. Sugahara, *Dalton Trans.*, 2022, **51**, 3625–3635.
112 A. I. B. Ivanov and P. A. Kralchevsky, *Colloids Surf., A*, 1997, **128**, 155–175.
113 B. J. A. Juárez and C. P. Whitby, *J. Colloid Interface Sci.*, 2012, **368**, 319–325.
114 T. Nakato, W. Ishitobi, M. Yabuuchi, M. Miyagawa, E. Mouri and Y. Yamauchi, *Langmuir*, 2021, **37**, 7789–7800.
115 M. Eguchi, M. S. Angelone, H. P. Yennawar and T. E. Mallouk, *J. Phys. Chem. C*, 2008, **112**, 11280–11285.
116 X. Wang, X. Ding and H. Zou, *Catalysts*, 2020, **10**, 12.
117 B.-C. Chen, H.-P. Lin, M.-C. Chao, C.-Y. Mou and C.-Y. Tang, *Adv. Mater.*, 2004, **16**, 1657–1661.
118 M. M. Tomczak, D. D. Glawe, L. F. Drummy, C. G. Lawrence, M. O. Stone, C. C. Perry, D. J. Pochan, T. J. Deming and R. R. Naik, *J. Am. Chem. Soc.*, 2005, **127**, 12577–12582.
119 H. Xie, Z. Li, L. Cheng, A. A. Haidry, J. Tao, Y. Xu, K. Xu and J. Z. Ou, *iScience*, 2022, **25**, 103598.
120 B. Jiang, Y. Guo, J. Kim, A. E. Whitten, K. Wood, K. Kani, A. E. Rowan, J. Henzie and Y. Yamauchi, *J. Am. Chem. Soc.*, 2018, **140**, 12434–12441.

This journal is © The Royal Society of Chemistry 2022